IOPscience iopscience.iop.org

Home Search Collections Journals About Contact us My IOPscience

Critical properties of S= 1/2 antiferromagnetic XXZ chain with next-nearest-neighbour interactions

This article has been downloaded from IOPscience. Please scroll down to see the full text article.

1994 J. Phys. A: Math. Gen. 27 5773

(http://iopscience.iop.org/0305-4470/27/17/012)

View the table of contents for this issue, or go to the journal homepage for more

Download details:
IP Address: 171.66.16.68
The article was downloaded on 01/06/2010 at 22:53

Please note that terms and conditions apply.

J. Phys. A: Math. Gen. 27 (1994) 5773–5788. Printed in the UK

Critical properties of $S = \frac{1}{2}$ antiferromagnetic XXZ chain with next-nearest-neighbour interactions

Kiyohide Nomura and Kiyomi Okamoto

Department of Physics, Tokyo Institute of Technology, Oh-okayama, Meguro-ku, Tokyo 152, Japan

Received 1 February 1994

Abstract. We investigate numerically the critical lines and the critical properties of the fluid–dimer and the Néel–dimer transitions of the $S = \frac{1}{2}$ antiferromagnetic XXZ chain with next-nearest interactions, and we confirm that the universality class of this model belongs to the quantum sine–Gordon model, as is expected from the bosonization. The method which we use in this paper to calculate the critical lines is free from the logarithmic corrections on the Kosterlitz–Thouless (K–T)-type transition line, which have made the K–T critical point difficult to obtain. By the use of this method, it is possible to determine the K–T critical line with high precision from small size data, and to identify the universality class.

1. Introduction

The $S = \frac{1}{2}$ antiferromagnetic XXZ chain with next-nearest-neighbour interactions is one of the typical models of competing interactions. This model is described by the following Hamiltonian:

$$H = \sum_{j=1}^{N}(S_j^x S_{j+1}^x + S_j^y S_{j+1}^y + \Delta S_j^z S_{j+1}^z) + \alpha \sum_{j=1}^{N}(S_j^x S_{j+2}^x + S_j^y S_{j+2}^y + \Delta S_j^z S_{j+2}^z) \tag{1}$$

where we assume the periodic boundary condition $S_{N+1} = S_1$, and N is the number of spins (N even). In this study we confine ourselves to the $\Delta \geqslant 0$ case.

For $\alpha = 0$ the ground-state properties are well known from the Bethe ansatz and the bosonization. In the region $0 \leqslant \Delta \leqslant 1$, the ground state is characterized by the gapless excitation and the power decay of the spin correlation. This state is called the spin-fluid state. When $\Delta > 1$, this system is Néel ordered and it has a twofold degenerate ground state separated from the excitation spectrum by a gap [1, 2]

$$\Delta E = \frac{\pi \sinh x}{x} \sum_{n=-\infty}^{n=\infty} \frac{1}{\cosh[(2n+1)\pi^2/2x]} \qquad (x = \cosh^{-1}\Delta)$$

$$\longrightarrow 4\pi\left(1 + \tfrac{1}{3}(\Delta - 1)\right) \exp\left(-\frac{\pi^2}{2\sqrt{2(\Delta - 1)}}\right) \qquad \text{for} \quad \Delta \to 1\,. \tag{2}$$

On the line $\alpha = \frac{1}{2}$, the exact ground state has been obtained [3–6]. Introducing the notation for the singlet pair :

$$[l, m] \equiv \frac{1}{\sqrt{2}}(\uparrow_l \downarrow_m - \downarrow_l \uparrow_m) \tag{3}$$

0305-4470/94/175773+16$19.50 © 1994 IOP Publishing Ltd

and defining $\Phi_1(N)$ and $\Phi_2(N)$ as

$$\Phi_1(N) \equiv [1,2][3,4]\ldots[N-1,N]$$
$$\Phi_2(N) \equiv [2,3][4,5]\ldots[N,1] \tag{4}$$

we can see that both $\Phi_1(N)$ and $\Phi_2(N)$ are eigenstates of the Hamiltonian (1) having energy

$$E_g(N) = -\tfrac{3}{8}NJ \tag{5}$$

when $\alpha = \frac{1}{2}$. The above energy $E_g(N)$ was proved to be the ground-state energy by van den Broek [5] and Shastry and Sutherland [6]. Note that the matrix element $\langle\Phi_1|\Phi_2\rangle$ vanishes as

$$\langle\Phi_1|\Phi_2\rangle = (-1)^{-N/2}2^{1-N/2} \tag{6}$$

so that the two states Φ_1, Φ_2 become orthogonal in the thermodynamic limit. Affleck *et al* [7] proved that only the states Φ_1, Φ_2 are the ground states and there is an energy gap between the ground state and the first excited state. Therefore the ground state is the purely dimerized state when $\alpha = \frac{1}{2}$. The dimer state is characterized by the excitation gap, the exponential decay of the spin correlation, and the dimer long-range order.

According to the above facts, there must exist a fluid–dimer transition line ($0 < \alpha_c(\Delta) < \frac{1}{2}$, $0 \leqslant \Delta \leqslant 1$) and a Néel–dimer transition line ($0 < \alpha_c(\Delta) < \frac{1}{2}$, $1 < \Delta$). With the bosonization technique used by Haldane [8] and Kuboki and Fukuyama [9], equation (1) is transformed into the quantum sine–Gordon model. At a glance, it may seem possible to determine the phase boundaries because the critical properties of the sine–Gordon model are well understood by use of the renormalization-group method. However, the mapping of (1) onto the sine–Gordon model is reliable only near $\Delta = 0$ and $\alpha = 0$, since the interaction couplings and the spin-wave velocity are renormalized and there is an ambiguity in the selection of the ultraviolet cut-off. Therefore we cannot correctly obtain the phase boundaries only by the bosonization. We must use the numerical results for the determination of the phase boundaries.

Tonegawa *et al* [10] diagonalized numerically the finite-size spin Hamiltonian (1). In order to determine the critical line $\alpha_c(\Delta)$, they applied the phenomenological renormalization group (PRG) method. But it is pointed out that in the case of the Kosterlitz–Thouless-type transition, the PRG method may lead to the wrong critical point [12] because of the irrelevant (marginal) operators.

In our previous papers [11, 12], we have obtained the phase diagram of this model, assuming that the low-energy excitations of (1) are described by the sine–Gordon model. In this paper we discuss the universality class of these transitions, and we confirm that the asymptotic long-distance behaviour of this model is described by the sine–Gordon model, as is expected.

In the phase diagram of the sine–Gordon model, there are the Gaussian fixed line and the Kosterlitz–Thouless (K–T)-type transition lines. At the K–T transition point, the divergence of the correlation length is not of the usual power-law type but very singular [13],

$$\xi \sim \exp(\text{constant} \times (\alpha - \alpha_c)^{-\sigma}). \tag{7}$$

In fact, all derivatives of the inverse of the correlation length at the critical point are zero. Also at the K–T critical point there appear the logarithmic corrections in various quantities, such as correlation functions and susceptibilities. Therefore it is very difficult to find the critical point of the K–T-type transition. One effective method to find this critical point is the Roomany–Wyld method [14], in which the β function is calculated numerically. We propose an efficient numerical method for determining the K–T critical point and its

universality class. We use the level crossings of the low excitations to determine the critical point. This idea is an extension of the method by Affleck *et al* [15]. Our method is better than the Roomany–Wyld method, as will be discussed in section 5.

This paper is organized as follows. In the next section, we explain how to determine the critical lines of the Hamiltonian (1), considering the symmetry of the low-lying excitations. In section 3, we calculate the critical exponents using the conformal field theory. In section 4, we discuss the asymptotic long-range behaviours expected from the sine–Gordon model and we confirm that the universality class of the model (1) is equivalent to that of the sine–Gordon model. In the last section, we compare our method with the phenomenological renormalization group method and the Roomany–Wyld method.

2. Critical points

We determine the critical points using the level crossing of the low-lying states with different symmetries. First let us consider the symmetry of the ground state and excited states.

The Hamiltonian (1) is invariant under spin rotation around the z-axis, translation ($S_i^z \to S_{i+1}^z$), space inversion ($S_i^z \to S_{N-i+1}^z$), and spin reversal ($S_i^z \to -S_i^z$). Then the corresponding eigenvectors have quantum numbers for the total spin ($m = \sum S_i^z$), the wavenumber ($q = 2\pi k/N$), the parity ($P = \pm 1$), and the spin reversal ($T = \pm 1$). For $N = 4n$, the ground state is the singlet ($m = 0, q = 0, P = 1, T = 1$) in the whole region. In the spin-fluid region, the first excited state is the doublet ($m = \pm 1, q = \pi, P = -1$). The energy gaps will disappear as $1/N$, and there is no energy gap in the thermodynamic limit. In the Néel region, the first excited state is the singlet ($m = 0, q = \pi, P = -1, T = -1$), which will be degenerate to the ground state as $\Delta E(N) \propto \exp(-\text{constant} \times N)$ in the $N \to \infty$ limit. Above the twofold degenerate ground state, there is an energy gap. In the dimer region, the first excited state is the singlet ($m = 0, q = \pi, P = 1, T = 1$), which becomes also degenerate to the ground state in the limit $N \to \infty$.

Thus the Néel–dimer transition is determined by the degeneracy between the Néel excitation ($m = 0, q = \pi, P = -1, T = -1$) and the dimer excitation ($m = 0, q = \pi, P = 1, T = 1$), and the fluid–dimer transition is characterized by the degeneracy between the doublet excitation ($m = \pm 1, q = \pi, P = -1$) and the dimer excitation, while the fluid–Néel transition by the degeneracy between the doublet and the Néel excitation. Note that for $N = 4n + 2$, the ground state is ($m = 0, q = \pi, P = -1, T = -1$), the doublet excitation ($m = \pm 1, q = 0, P = 1$), the dimer excitation ($m = 0, q = 0, P = -1, T = -1$), and the Néel excitation ($m = 0, q = 0, P = 1, T = 1$).

On the basis of the above symmetry consideration, we analyse the numerical data. First we consider the Néel–dimer transition. In figure 1 we show the Néel, the dimer, and the doublet excitations ($\Delta = 2.0, N = 20$). Note that the dimer and the Néel excitations cross linearly. As mentioned above, we can determine the critical point $\alpha_c(\Delta, N)$ by the crossing point of the Néel and dimer excitations. In figure 2, we plot $\alpha_c(\Delta, N)$ as a function of the system size. It is seen from figure 2 that the crossing points $\alpha_c(\Delta, N)$ are almost independent of the system size, and that the remaining correction is $O(N^{-2})$

$$\alpha_c(\Delta, N) = \alpha_c(\Delta) + \text{constant} \times N^{-2}. \tag{8}$$

This $O(N^{-2})$ correction is due to the irrelevant field whose scaling dimension is $x = 4$. This irrelevant field, which does not exist in the pure sine–Gordon model, comes from the nonlinear term neglected when linearizing the dispersion relation near the Fermi level in the course of the bosonization. We will explain in section 4, on the basis of the sine–Gordon

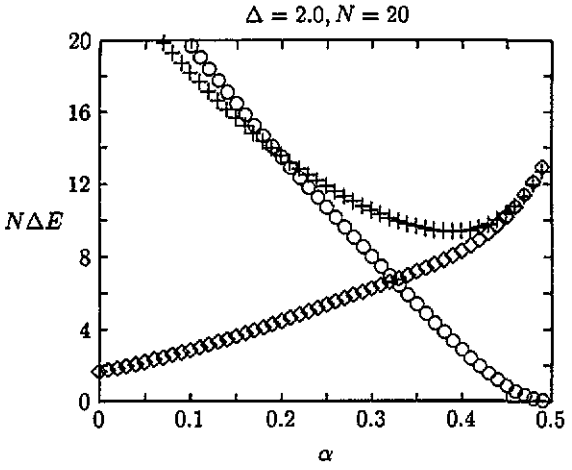

Figure 1. The Néel (◇), dimer (○), and the doublet (+) excitations in the Néel and dimer region (Δ = 2.0).

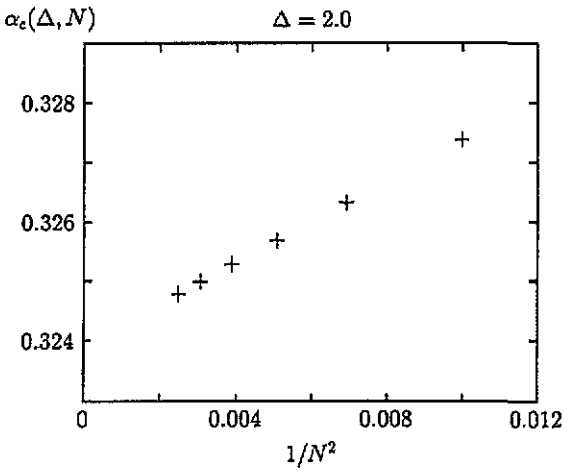

Figure 2. The crossing points $\alpha_c(\Delta, N)$ of the Néel and dimer excitations as a functon of the system size N.

model, the reason that the crossing point of the dimer and the Néel excitations is indeed the critical point and that both excitations cross linearly.

Next we consider the dimer–fluid transition. In figure 3 we show the Néel, the dimer, and the doublet excitations ($\Delta = 0.5, N = 20$). It is seen from figure 3 that the dimer and the doublet excitations cross linearly and in this case the dimer and Néel excitations also cross linearly. As mentioned above, we can determine the dimer–fluid critical point $\alpha_c(\Delta, N)$ by the crossing point of the doublet and dimer excitations. In figure 4, we plot $\alpha_c(\Delta, N)$ as a function of the system size. Also in this case the crossing points $\alpha_c(\Delta, N)$ obey (8). Note that the crossing points of the Néel and the dimer excitations in the spin-fluid region obey (8), too. This is not the critical point, but this is the Gaussian fixed point ($y_\phi = 0$) as we shall discuss in section 4.

Finally about the Néel–fluid transition point, the crossing points of the Néel and doublet excitations always stay at $\Delta = 1$ because of the $SU(2)$ symmetry of the Hamiltonian (1) itself on this line.

In summary the whole phase diagram is shown in figure 5, where critical points are extrapolated using (8).

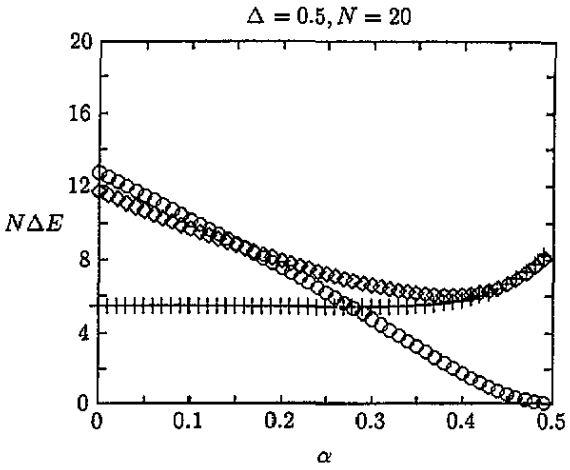

Figure 3. The Néel (◇), dimer (○) and the doublet (+) excitations in the dimer and spin–fluid region ($\Delta = 0.5$).

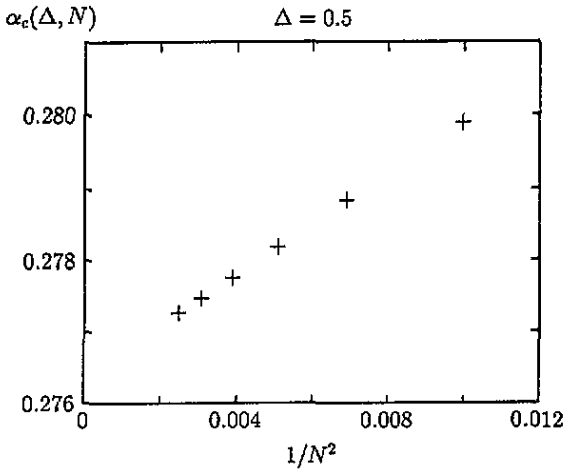

Figure 4. The crossing points $\alpha_c(\Delta, N)$ of the dimer and doublet excitatons as a function of the system size N.

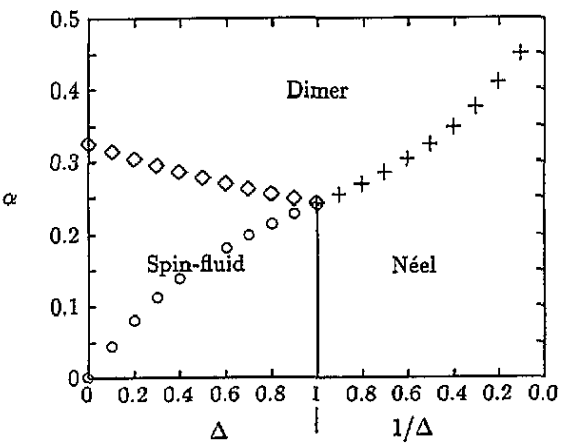

Figure 5. The phase diagram of the present model (1). (+) Néel–dimer critical points; (◇) dimer–fluid critical points; (○) Gaussian fixed points.

3. Critical exponents by the conformal field theory

Conformal field theory [16, 17] is a powerful method to determine the critical dimensions of the two-dimensional classical system which is scale invariant, that is, at the critical fixed

point. It also describes the one-dimensional massless quantum system at $T = 0$. One important result of the conformal field theory is the relation between the critical dimensions and the energy gaps of the finite-size system with periodic boundary conditions [18]

$$E_n(N) - E_0(N) = \frac{2\pi v x_n}{N} \tag{9}$$

where x_n is the critical dimension and is related to the critical exponent η of the corresponding correlation function as $2x = \eta$, and v is the spin-wave velocity for the model. The other important formula is the finite-size correction to the ground-state energy [19,20]

$$E_0(N) = \epsilon_0 N - \frac{\pi v c}{6N} \tag{10}$$

where c is the conformal anomaly number which plays a central role in the conformal field theory.

At first we must calculate the spin-wave velocity. The spin-wave velocity can be obtained from the energy gap at the wavenumber $k = 2\pi/N$ as

$$v = \frac{N\Delta E(k = 2\pi/N)}{2\pi} \tag{11}$$

and extrapolating this to the thermodynamic limit. Using this velocity and (10), we obtain the conformal anomaly $c = 1$ within a few per cent (see figure 6).

In the course of the calculation of the spin-wave velocity and other critical dimensions, the difficult problem is to estimate the finite-size corrections to them. Unfortunately, the explicit formula for the correction of the spin-wave velocity (11) is unknown. For the critical dimension, the correction from the irrelevant field x' ($x' > 2$) to (9) is obtained by the perturbation as $O(N^{2-x'})$ [21]. Also, for the conformal anomaly, since the first-order perturbation term disappears by the symmetry, the remaining correction is $O(N^{4-2x'})$ and the amplitude of this term is small [22]. However, for the irrelevant operator $L_{-2}\bar{L}_{-2}\mathbf{1}$, which is the descendant of the identity operator $\mathbf{1}$ and which has a scaling dimension $x = 4$, the first-order perturbation to the ground-state energy remains and the amplitude of this term is larger than other terms. Hence this $x = 4$ correction gives the main contribution in many cases. Therefore, assuming the conformal anomaly $c = 1$, we will use the following equation:

$$E_0(N) = \epsilon_0 N - \frac{\pi v}{6N}(1 + O(N^{-2})) \tag{12}$$

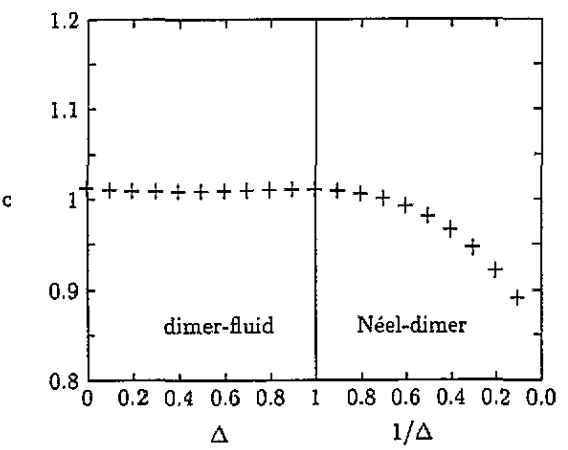

Figure 6. The conformal anomaly c (10) on the fluid–dimer and Néel–dimer critical lines. Here we use the spin-wave velocity obtained from (11).

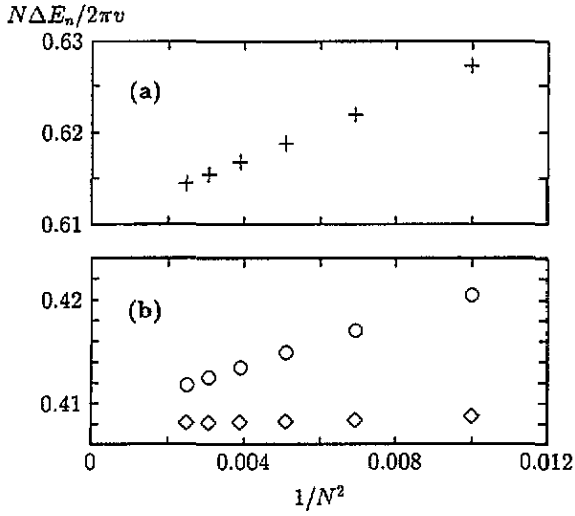

Figure 7. The values of $N\Delta E_n/2\pi v$ (ΔE_n : energy gap) for the Néel, dimer, doublet excitations as a function of system size N. (*a*) doublet, (*b*) Néel (◇) and dimer (○) excitations.

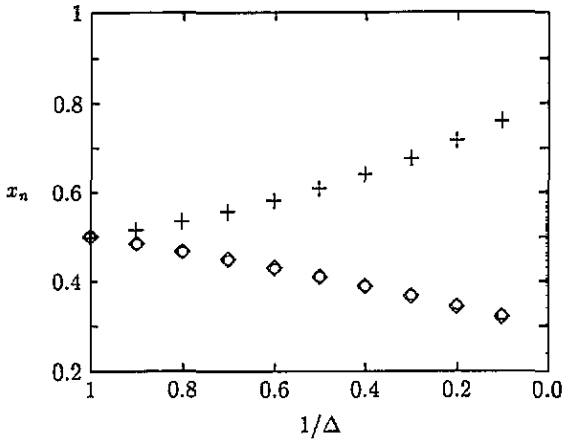

Figure 8. The critical dimensions for the Néel (◇), dimer (○), doublet (+) excitations.

in order to obtain the spin-wave velocity. As will be shown in section 4, the spin-wave velocity calculated by this method is more accurate than that from (11).

Next we consider the critical dimensions. In general, there are the corrections from the irrelevant operators and it is difficult to eliminate them. However, as we shall explain in the next section, on the Néel–dimer line there are no irrelevant fields within the sine–Gordon theory, and there is only the $x = 4$ irrelevant field which is not included in the sine–Gordon model. Thus critical dimensions can be obtained as

$$E_n(N) - E_0(N) = \frac{2\pi v x_n}{N}(1 + O(N^{-2})) \tag{13}$$

(see figure 7). In figure 8 we show the critical dimensions for the Néel, dimer and doublet excitations. Note that these critical exponents vary continuously as the anisotropy Δ changes, which is typical for the $c = 1$ conformal field theory [23].

On the dimer–fluid (or the Néel–fluid) transition line, there are the logarithmic corrections from the marginally irrelevant field. However, the ratios of the logarithmic corrections in the several low-energy excitations can be obtained from conformal field theory [15], which enables us to eliminate the logarithmic corrections. We will treat this point in the next section.

4. Sine–Gordon model and universality class

In this section we review the renormalization-group properties of the sine–Gordon model and explain why the crossing of the low-energy excitations is linear and investigate the universality class of this model (1).

With the bosonization technique used by Haldane [8], and Kuboki and Fukuyama [9], equation (1) is transformed into the quantum sine–Gordon model:

$$H = \frac{1}{2\pi}\int \mathrm{d}x \left[(uK)(\pi\Pi)^2 + \left(\frac{u}{K}\right)(\partial_x\phi)^2\right] + \frac{2g_\phi}{(2\pi a)^2}\int \mathrm{d}x \cos\sqrt{8}\phi \tag{14}$$

where the commutation relation

$$[\phi(x), \Pi(x')] = \mathrm{i}\delta(x - x') \tag{15}$$

holds, and a is the lattice constant. The coefficients u, K and g_ϕ are related to α, Δ as

$$u = 2\sqrt{AC} \qquad K = \frac{-1}{2\pi}\sqrt{\frac{C}{A}} \qquad g_\phi = -2\pi^2 a^2 D \tag{16}$$

where

$$\begin{aligned} A &= \frac{a}{8\pi}\left(1 + \frac{3\Delta}{\pi} + \frac{(6+\Delta)\alpha}{\pi}\right) \\ C &= 2\pi a\left(1 - \frac{\Delta}{\pi} - \frac{(2-\Delta)\alpha}{\pi}\right) \\ D &= \frac{1}{2a}(\Delta - (2+\Delta)\alpha)\ . \end{aligned} \tag{17}$$

It is seemingly easy to determine the phase boundaries because the critical properties of the sine–Gordon model are well understood by use of the renormalization-group method. However, the expressions for the coefficients (A, C, D) are reliable only near $\Delta = 0$ and $\alpha = 0$. Therefore we cannot correctly obtain the phase boundaries themselves from (16) and (17), although the critical properties are qualitatively well expressed by the sine–Gordon model. We must use the numerical results for the determination of the phase boundaries. However, there are the corrections from the irrelevant fields which make the extrapolation of the finite-size results very difficult. Then we first review the renormalization properties of the sine–Gordon model and we explain the method to avoid the correction from the irrelevant fields.

The renormalization-group equations for the sine–Gordon Hamiltonian (14) up to the lowest order in y_0 and y_ϕ are

$$\frac{\mathrm{d}y_0(l)}{\mathrm{d}l} = -y_\phi^2(l) \qquad \frac{\mathrm{d}y_\phi(l)}{\mathrm{d}l} = -y_\phi(l)y_0(l) \tag{18}$$

where

$$y_0(0) = \frac{g_0}{\pi u} \qquad y_\phi(0) = \frac{g_\phi}{\pi u} \qquad K = 1 + \frac{g_0}{2\pi u}\ . \tag{19}$$

The flow diagram of (18) is shown in figure 9. For the finite spin system, l is related to N by $\mathrm{e}^l = N$. Note that there are three critical lines: that is, $y_\phi = 0$ ($y_0 < 0$) corresponding to the Néel–dimer transition line, $y_\phi = -y_0$ ($y_0 > 0$) to the fluid–Néel transition line, and $y_\phi = y_0$ ($y_0 > 0$) to the fluid–dimer transition line.

First we explain the reason why the difference of the dimer and Néel excitations is linear near the Néel–dimer transition line, etc. According to Giamarchi and Schulz [24],

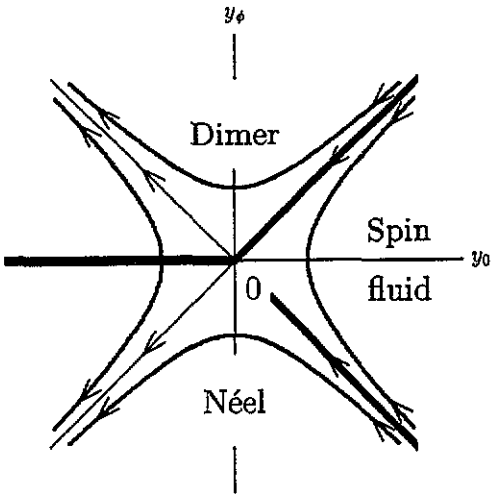

Figure 9. The flow diagram of the renormalization (18) on the y_0–y_ϕ plane. The phase boundaries are shown by the thick lines.

the correlation functions

$$\begin{aligned} R_0 &\equiv 2\langle T_\tau \cos(\sqrt{2}\phi(r_1))\cos(\sqrt{2}\phi(r_2))\rangle & R_1 &\equiv 2\langle T_\tau \cos(\sqrt{2}\theta(r_1))\cos(\sqrt{2}\theta(r_2))\rangle \\ R_2 &\equiv 2\langle T_\tau \sin(\sqrt{2}\theta(r_1))\sin(\sqrt{2}\theta(r_2))\rangle & R_3 &\equiv 2\langle T_\tau \sin(\sqrt{2}\phi(r_1))\sin(\sqrt{2}\phi(r_2))\rangle \end{aligned} \tag{20}$$

are expressed by the renormalized quantities $y_0(l)$, $y_\phi(l)$ as

$$\begin{aligned} R_0 &= \exp\left[-\int_0^{\ln(r/a)} \mathrm{d}l\left(1+\tfrac{1}{2}y_0(l)+y_\phi(l)\right)\right] \\ R_1 = R_2 &= \exp\left[-\int_0^{\ln(r/a)} \mathrm{d}l\left(1-\tfrac{1}{2}y_0(l)\right)\right] \\ R_3 &= \exp\left[-\int_0^{\ln(r/a)} \mathrm{d}l\left(1+\tfrac{1}{2}y_0(l)-y_\phi(l)\right)\right] \end{aligned} \tag{21}$$

where $\theta(x)$ is a dual field of $\phi(x)$ defined as $\pi\Pi(x) \equiv \partial_x\theta(x)$. The renormalized critical exponents $\eta_i(l)$ are related to the correlation functions by [25]

$$R_i = \exp\left[-\int_0^{\ln(r/a)} \mathrm{d}l\,\eta_i(l)\right] \tag{22}$$

and by the use of (9), which relates the critical exponent η to the energy gap for the finite-size system, we obtain

$$\frac{N\Delta E_i}{2\pi v} = x_i(l) = \tfrac{1}{2}\eta_i(l) \tag{23}$$

so that the differences between the energy gaps become

$$\begin{aligned} x_0(l) - x_1(l) &= \tfrac{1}{2}[y_0(l)+y_\phi(l)] \\ x_0(l) - x_3(l) &= y_\phi(l) \\ x_3(l) - x_1(l) &= \tfrac{1}{2}[y_0(l)-y_\phi(l)]. \end{aligned} \tag{24}$$

Although (9) is satisfied under the condition of scale invariance, by the use of the renormalization group, we extend this relation to the region where scale invariance is not strictly satisfied but the system size is sufficiently smaller than the correlation length ξ of the $N \to \infty$ limit.

Therefore the differences of the low-energy excitations are linear with the distance from the critical lines and these are the good quantities to determine the critical lines. Note that the fast varying parts of the spin operators are expressed by $\theta(x), \phi(x)$ as

$$S_x^+ \propto e^{i\pi x} e^{-i\sqrt{2}\theta(x)} \qquad S_x^z \propto e^{i\pi x} \cos\left[\sqrt{2}\phi(x)\right] \tag{25}$$

and

$$S_x^+ S_{x+1}^- + S_x^- S_{x+1}^+ \propto e^{i\pi x} \sin\left[\sqrt{2}\phi(x)\right] \tag{26}$$

respectively. Then the correlations R_0, $R_1 = R_2$, R_3 correspond to the Néel, doublet dimer correlations, respectively.

At this stage we consider the universality class on the Néel–dimer transition line ($y_\phi = 0$). On this line the critical exponents vary continuously as shown in figure 8, which is natural from the viewpoint of the sine–Gordon picture. However, when we assume the Gaussian model, it is well known that there is only one parameter which governs these critical exponents. The relation of the critical dimensions corresponding to the $q = \pi$ excitations ($N = 4n$ case) is written as

$$x_{\text{dimer}} = x_{\text{neel}} \tag{27}$$

$$x_{\text{doublet}} x_{\text{dimer}} = \tfrac{1}{4} \tag{28}$$

because the doublet, Néel and dimer correlations behave as

$$\begin{aligned} &\langle S_r^+ S_0^- \rangle \propto e^{i\pi r} \langle \exp(-i\sqrt{2}\theta(r)) \exp(i\sqrt{2}\theta(0)) \rangle \propto e^{i\pi r} r^{-1/K} \\ &\langle S_r^z S_0^z \rangle \propto e^{i\pi r} \langle \cos(\sqrt{2}\phi(r)) \cos(\sqrt{2}\phi(0)) \rangle \propto e^{i\pi r} r^{-K} \\ &\langle (S_0^+ S_1^- + S_0^- S_1^+)(S_r^+ S_{r+1}^- + S_r^- S_{r+1}^+) \rangle \propto e^{i\pi r} \langle \sin(\sqrt{2}\phi(r)) \sin(\sqrt{2}\phi(0)) \rangle \propto e^{i\pi r} r^{-K} \end{aligned} \tag{29}$$

and the relation $\eta = 2x$.

There are also relevant, marginal and irrelevant fields corresponding to the $q = 0$ excitations ($N = 4n$ case). The critical dimensions corresponding to them satisfy the following relation [26]:

$$x_{\text{rel}} = 4x_{\text{neel}} \tag{30}$$

$$x_{\text{marg}} = 2 \tag{31}$$

$$x_{\text{irrel}} = 4x_{\text{doublet}}\,. \tag{32}$$

The x_{rel} is related with the mass-gap generation near the Néel–dimer critical line. The reason is as follows. Considering the case of $y_\phi(l) \ll 1$, $y_0(l) < 0$ and the renormalization equations(18), we obtain

$$y_\phi(l) = y_\phi(0) \exp[-y_0(0) l]\,. \tag{33}$$

In the neighbourhood of the critical line, the correlation length ξ is defined as the value $\xi \sim e^l$ for which $y_\phi(l)$ becomes of order unity. Hence,

$$\ln y_\phi(0) = y_0(0) \ln \xi \tag{34}$$

from which the critical exponent ν ($\xi \equiv y_\phi(0)^{-\nu}$) becomes

$$\frac{1}{\nu} = -y_0(0)\,. \tag{35}$$

The scaling dimension x_{rel} and ν are related by [22]

$$\frac{1}{\nu} = 2 - x_{\text{rel}}\,. \tag{36}$$

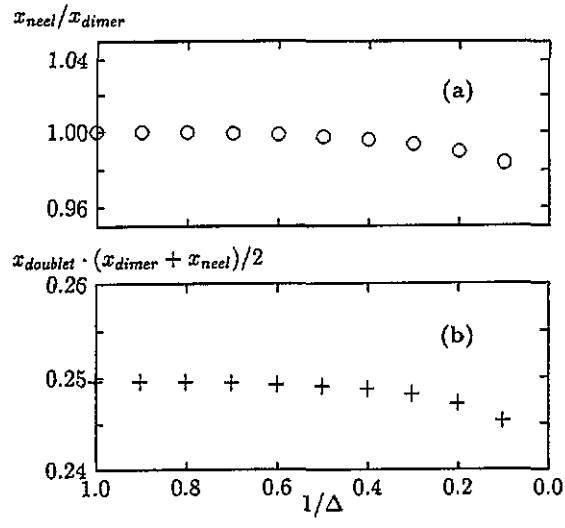

Figure 10. The one-parameter scaling relation of the $q = \pi$ excitations. (*a*) The ratios x_{neel}/x_{dimer}; (*b*) the products $x_{doublet}(x_{neel} + x_{dimer})/2$ for various anisotropies.

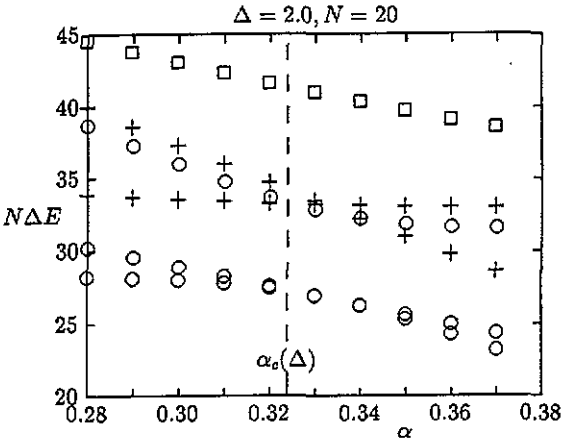

Figure 11. The excitation spectrum at $q = 0$ near the Néel–dimer critical point $\alpha_c(\Delta)$. (○) $S_z^{tot} = 0$ excitation; (+) $S_z^{tot} = \pm 1$ excitation; (□) $S_z^{tot} = \pm 2$ excitation.

From (19) and (30), we see that, $K = 1 + y_0/2 = 2x_{neel}$, to obtain

$$x_{rel} = 4x_{neel}\,. \tag{37}$$

There are also marginal fields $x = 2$ so that along the Néel–dimer critical line there is no mass generation and the critical exponents are varying continuously due to this field [26].

Now we check whether these relations hold for the critical dimensions obtained in section 3. In figure 10, we show the ratios x_{neel}/x_{dimer} and the products $x_{doublet}(x_{neel} + x_{dimer})/2$ at various anisotropies Δ. We show the excitation spectra at $q = 0$ in the neighbourhood of the Néel–dimer critical line in figure 11. There are the twofold degenerate $S_z^{tot} = 0$ state corresponding to x_{rel}, the twofold $S_z^{tot} = \pm 1$ and one $S_z^{tot} = 0$ state to x_{marg}, and one $S_z^{tot} = \pm 2$ state to x_{irrel}. In figure 12, we also show the ratio $2x_{rel}/(x_{neel} + x_{dimer})$, $x_{irrel}/x_{doublet}$ and the marginal fields x_{marg} at various anisotropies. The one-parameter scaling relations for the Gaussian model hold in high accuracy. Therefore we conclude that this critical line belongs to the Gaussian universality class.

At last we consider the universality class on the fluid–dimer critical line. There are the logarithmic corrections which make the extrapolation of the critical exponents very difficult.

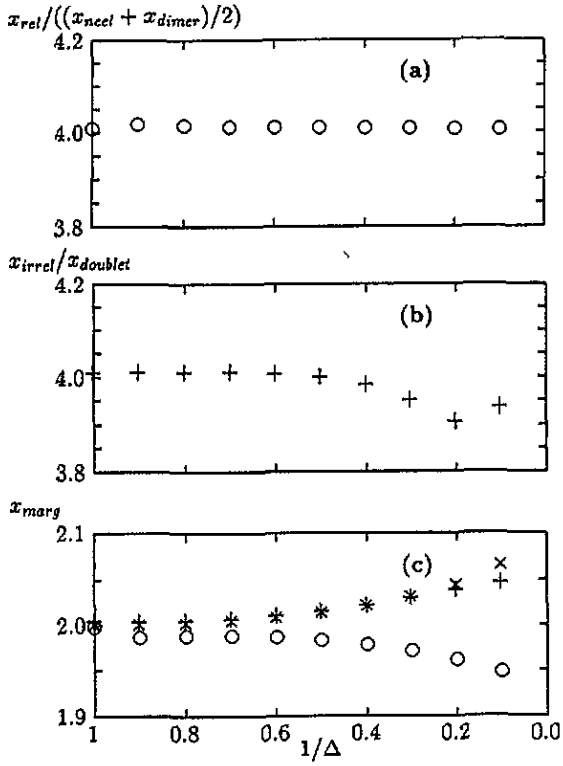

Figure 12. The one-parameter scaling relation of the $q = 0$ excitations. (*a*) The ratio $x_{\rm rel}/((x_{\rm neel} + x_{\rm dimer})/2)$; (*b*) the ratio $x_{\rm irrel}/x_{\rm doublet}$; (*c*) the marginal $x_{\rm marge}$. (○) $S_z^{\rm tot} = 0$, (+) $S_z^{\rm tot} = \pm 1$, (×) $S_z^{\rm tot} = \pm 1$; for various anisotropies.

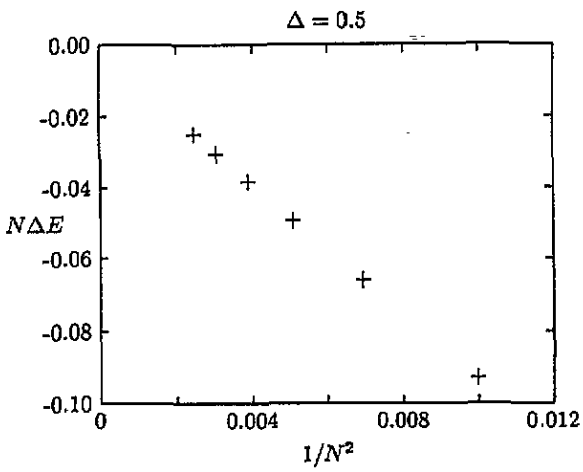

Figure 13. The energy difference ΔE between the dimer and doublet excitation on the dimer–fluid critical line. The $N\Delta E$ converges as $1/N^2$, and this means that the $SU(2)$ symmetry appears.

But in the case of the $\beta^2 = 8\pi$ sine–Gordon model, which is equivalent to the $SU(2)$ $k = 1$ Wess–Zumino–Witten model [27], the ratios of the logarithmic corrections can be obtained [20] so that it is possible to eliminate them by the use of the several low excitations [28]. That is,

$$x_1(l) = x_2(l) = x_3(l) = \frac{1}{2} - \frac{1}{4}\frac{1}{\ln N} \tag{38}$$

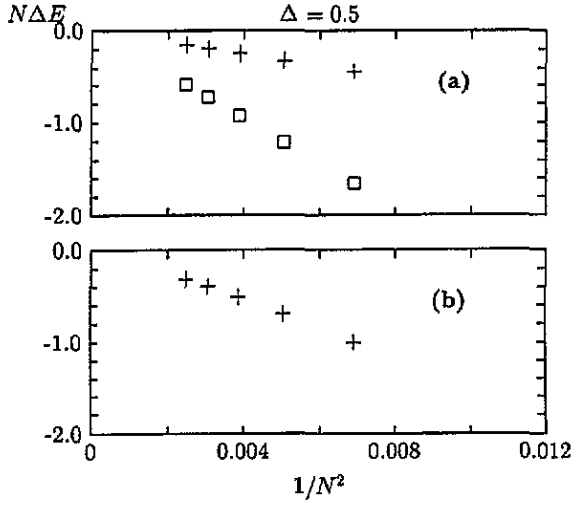

Figure 14. The enegy difference ΔE at $q = 0$ excitations. (*a*) The energy gap of $S_z^{\rm tot} = \pm 2$, $S_z^{\rm tot} = \pm 1$ states measured from $S_z^{\rm tot} = 0$ excitation. (*b*) The energy gap of $S_z^{\rm tot}$+± 1 states measured from $S_z^{\rm tot} = 0$. The $N\Delta E$ converges as $1/N^2$, and this means that the $SU(2)$ symmetry appears.

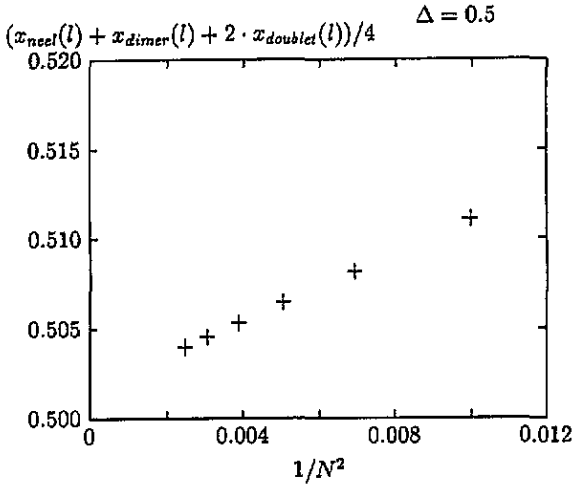

Figure 15. The average, $(x_{\rm neel}(l) + x_{\rm dimer}(l) + 2x_{\rm doublet}(l))/4$, as a function of system size.

$$x_0(l) = \frac{1}{2} + \frac{3}{4}\frac{1}{\ln N} \tag{39}$$

which enables us to eliminate logarithmic corrections using the average of $(x_{\rm neel}(l) + x_{\rm dimer}(l) + 2x_{\rm doublet}(l))/4$.

We check whether these relation hold for the critical dimensions. In figure 13 we show the energy difference between the dimer and doublet excitations as a function of the system size ($\Delta = 0.5$). It converges to zero with $1/N^2$ due to the $x = 4$ irrelevant field. We also check the $SU(2)$ symmetry at $q = 0$ excitations for $S_z^{\rm tot} = 0, \pm 1, \pm 2$ in figure 14 (there are three $S_z^{\rm tot} = 0$, two $S_z^{\rm tot} = \pm 1$, one $S_z^{\rm tot} = \pm 2$ excitations which correspond to the $x = 2$ critical dimension). This means that on this critical line, within the limit of the sine–Gordon model, the $SU(2)$ symmetry appears by the renormalization which does not exist in the original Hamiltonian (1).

In figure 15, we show the average $(x_{\rm neel}(l) + x_{\rm dimer}(l) + 2x_{\rm doublet}(l))/4$ as a function of the system size. It converges to $x = \frac{1}{2}$ as expected. The remaining correction is due to the $x = 4$ irrelevant field. In figure 16 we show the extrapolated average for various anisotropy

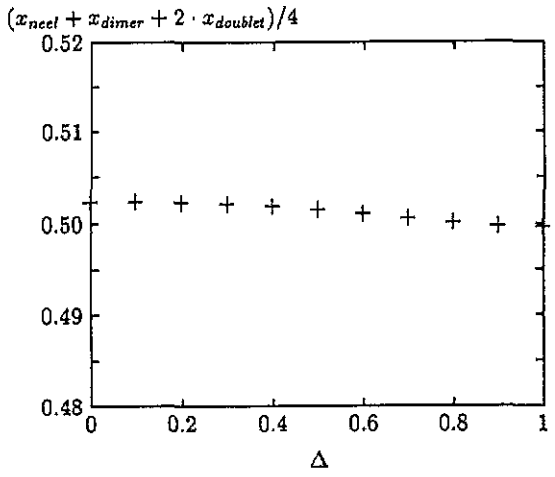

Figure 16. The extrapolated average, $(x_{\text{ncel}} + x_{\text{dimer}} + 2x_{\text{doublet}})/4$, on the dimer–fluid critical line. The logarithmic corrections are cancelled out.

Δ. Therefore we conclude that this critical line belongs to the $\beta^2 = 8\pi$ sine–Gordon model (which has an $SU(2)$ symmetry) universality class.

5. Discussions

Our idea that the level crossings of the low excitations can be used to determine the critical point is developed from the work by Affleck *et al* [15], who studied the isotropic XXX case for this problem on the basis of the conformal field theory and the renormalization group. But it is not clear in their work how to determine the Kosterlitz–Thouless (K–T)-type critical point for the anisotropic case. Furthermore, they did not point out that the difference of the low-energy excitations is proportional to the distance from the critical point, which makes it easier to determine the critical points.

In the following we compare our method with the other methods to analyse the K–T-type transition from the finite-size calculations.

First we point out that the phenomenological renormalization-group calculation, which is useful for the second-order transition, leads to the false conclusion in the K–T-type transition. Tonegawa, Harada and Kaburagi (THK) [10] diagonalized numerically the finite-size spin Hamiltonian (1). In order to determine the critical line $\alpha_c(\Delta)$, they applied the phenomenological renormalization group (PRG) equation,

$$(N+2)\Delta E(N+2, \alpha_c(\Delta, N+1)) = N\Delta E(N, \alpha_c(\Delta, N+1)) \tag{40}$$

and extrapolated $\alpha_c(\Delta, N)$ to $\alpha_c(\Delta, \infty)$. For $\Delta E(N)$, they used the singlet–doublet energy gap for the N spin chain,

$$\Delta E_{sd}(N) \equiv E_1^{(0)}(N) - E_0^{(0)}(N) \tag{41}$$

where $E_m^{(0)}(N)$ and $E_m^{(l)}(N)$ are the lowest energy and the lth excited energy in the $\sum_j S_j^z = m$ space, respectively. For the isotropic case ($\Delta = 1$), their result of $\alpha_c = 0.25$ is consistent with $\alpha_c = 0.2411 \pm 0.0001$ determined by Okamoto and Nomura [11]. Furthermore, their Néel–dimer critical line is almost the same as ours. But with the dimer–fluid transition line $\alpha_c(\Delta)$, THKs $\alpha_c(\Delta)$ decreases as Δ decreases, in contrast to our results where $\alpha_c(\Delta)$ increases as Δ decreases.

The reason for this difference is explained as follows. In the spin–fluid region, the $\cos\sqrt{8}\phi$ term is renormalized to zero as $N \to \infty$. Therefore the PRG relation (40) is

satisfied in the lowest approximation and the irrelevant operators become important in determining the PRG solution. As is clear from the sine–Gordon Hamiltonian (14), the PRG relation holds best when $g_\phi = 0$ (i.e. $y_\phi = 0$). In real cases, the PRG relation may have a solution near $y_\phi = 0$, because there may exist irrelevant operators other than the $\cos\sqrt{8}\phi$ term, as already stated. Since the fluid–dimer transition is determined by $y_\phi = y_0$, the PRG solution yields a smaller value of y_ϕ for the fluid–dimer transition. Further, using (16) and (17), we can see that the PRG solution brings about a value of $\alpha_c(\Delta)$ smaller than the correct value. Thus the difference between our fluid–dimer line and that of THK is clearly explained.

Here we demonstrate that the PRG solution may lead to an incorrect critical point for the K–T-type transition. When $\alpha = 0$, as is well known, Hamiltonian (1) has the fluid–Néel critical point of the K–T-type at $\Delta = 1$. If we apply the PRG method to the finite-size numerical data, we obtain $\Delta_c = 0.50706$ $(N = 10, 12)$ and $\Delta_c = 0.47654$ $(N = 18, 20)$. Therefore the critical value Δ_c obtained by the PRG equation is far from the exact value $\Delta = 1$. Then, the PRG analysis is dangerous for the K–T-type transitions.

As for the Néel–dimer transition, the phase transition is from the finite-gap Néel phase to the finite-gap dimer phase, and only on the Néel–dimer transition line is the excitation gapless. In this case the PRG equation produces correct results.

Next we compare our method with the Roomany–Wyld method [14] which has been the most reliable method to treat the K–T-type transition. In the Roomany–Wyld method, the critical point is determined by the zero point of the β-function. As for the second-order transition, the β-function linearly crosses the zero point

$$\beta(g) \simeq (g - g^*)/\nu\,. \tag{42}$$

In the case of the K–T-type transition, the β-function vanishes higher than the first order from the disordered region, and always zero in the power-law decaying region.

$$\beta(g) = \begin{cases} \sim (g - g^*)^{1+\sigma} & g > g^* \quad g \to g^* \\ \equiv 0 & g < g^* \end{cases} \tag{43}$$

where σ is defined in (7). Therefore the accuracy to determine the critical point is less than our method, where near the critical point the quantity $x_0(l) - x_1(l)$ $(x_3(l) - x_1(l))$ crosses zero linearly.

Furthermore, in order to obtain the critical exponents, the curvature of the β-function is used in the Roomany–Wyld method. However, this quantity is affected by the logarithmic corrections, which bring about an uncertainty for the calculation of the critical exponents. By using the method proposed by Ziman and Schulz [28], the logarithmic corrections of the critical dimensions can be canceled out, so the problem of the logarithmic correction is avoided.

In conclusion, we could not only obtain the critical lines with high accuracy, but also we could verify that the universality class of this model (1) belongs to the sine–Gordon model, as expected by the bosonization.

Acknowledgments

We would like to express our appreciation to Dr Sakai and Dr Nonomura for the discussions on the Roomany–Wyld method. We also thank Professors T Tonegawa, I Harada, and M Kaburagi for sending us their preprints and reprints. For the numerical calculation, we used the computer program TITPACK version 2 developed by Professor H Nishimori, to whom we are greatly indebted. This work was partly supported by a Grant-in-Aid

for Scientific Research on Priority Areas, 'Computational Physics as a New Frontier in Condensed Matter Research', from the Ministry of Education, Science and Culture, Japan. The numerical calculations were performed on supercomputers in the Computer Center of the University of Hokkaido.

References

[1] des Cloizeaux J and Gaudin M 1966 *J. Math. Phys.* **7** 1384
[2] Yang C N and Yang C P 1966 *Phys. Rev.* **151** 258
[3] Majumdar C K and Ghosh D K 1969 *J. Math. Phys.* **10** 1399
[4] Majumdar C K 1970 *J. Phys. C: Solid State Phys.* **3** 911
[5] van den Broek P M 1980 *Phys. Lett.* **77A** 261
[6] Shastry B S and Sutherland B 1981 *Phys. Rev. Lett.* **47** 964
[7] Affleck I, Kennedy T, Lieb E H and Tasaki H 1988 *Commun. Math. Phys.* **115** 477
[8] Haldane F D M 1982 *Phys. Rev.* B **25** 4925; **26** 5257 (Erratum)
[9] Kuboki K and Fukuyama H 1987 *J. Phys. Soc. Japan* **56** 3126
[10] Tonegawa T, Harada I and Kaburagi M 1992 *J. Phys. Soc. Japan* **61** 4665
[11] Okamoto K and Nomura K 1992 *Phys. Lett.* **169A** 433
[12] Nomura K and Okamoto K 1993 *J. Phys. Soc. Japan* **62** 1123
[13] Kosterlitz J M and Thouless D J 1973 *J. Phys. C: Solid State Phys.* **6** 1181
Kosterlitz J M 1974 *J. Phys. C: Solid State Phys.* **7** 1046
[14] Roomany H H and Wyld H W 1980 *Phys. Rev.* D **21** 3341; 1981 *Phys. Rev.* B **23** 1357
[15] Affleck I, Gepner D, Schulz H J and Ziman T 1989 *J. Phys. A: Math. Gen.* **22** 511
[16] Belavin A A, Polyakov A M and Zamolodchikov A B 1984 *Nucl. Phys.* B **241** 333
[17] Friedan D, Qiu Z and Shenker S H 1984 *Phys. Rev. Lett.* **52** 1575
[18] Cardy J L 1984 *J. Phys. A: Math. Gen.* **17** L385
[19] Blöte H W J , Cardy J L and Nightingale M P 1986 *Phys. Rev. Lett.* **56** 742
[20] Affleck I 1986 *Phys. Rev. Lett.* **56** 746
[21] Cardy J L 1986 *Nucl. Phys.* B **270** [FS 16] 186
[22] Cardy J L 1986 *J. Phys. A: Math. Gen.* **19** L1093; 1987 *J. Phys. A: Math. Gen.* **20** 5039(E)
[23] Cardy J L 1987 *J. Phys. A: Math. Gen.* **20** L891
[24] Giamarchi T and Schulz H J 1989 *Phys. Rev.* B **39** 4620
[25] Amit D J 1984 *Field Theory, the renormalization-group, and Critical Phenomena* (Singapore: World Scientific)
[26] Kadanoff L P and Brown A C 1979 *Ann. Phys., NY* **121** 318
[27] Affleck I 1986 *Nucl. Phys.* B **265** [FS15] 448
[28] Ziman T A L and Schulz H J 1987 *Phys. Rev. Lett.* **59** 140